International Journal of Robotics and Control Systems
Vol. 6, No. 2, 2026, pp. 870-887
ISSN 2775-2658
http://pubs2.ascee.org/index.php/ijrcs

A Traceability-Oriented Integration Framework for Automated Optical Inspection and Barcode-Assisted Warehousing in SMT Production

Minh B. Lam [a,1], Trung-Nhan Nguyen [a,2,*], Thanh-Quyen Ngo [a,3], Van-Sy Nguyen [a,4], Trung-Tin V. Phan [a,5], Dinh-Khoi Hoang [a,6]

[a] Faculty of Electrical Engineering Technology, Industrial University of Ho Chi Minh City, Ho Chi Minh City, Vietnam
[1] lambinhminh@iuh.edu.vn; [2] nguyentrungnhan@iuh.edu.vn; [3] ngothanhquyen@iuh.edu.vn; [4] nguyenvansy@iuh.edu.vn; [5] trungtin8947@gmail.com; [6] hoangdinhkhoi@iuh.edu.vn
* Corresponding Author

ARTICLE INFO

Article history
Received January 26, 2026
Revised March 12, 2026
Accepted April 01, 2026

Keywords
Surface-Mount Technology;
Automated Optical Inspection;
Supervisory Integration;
Barcode-Assisted Warehousing;
Printed Circuit Boards

ABSTRACT

In conventional surface-mount technology (SMT) production lines, automated optical inspection (AOI) and warehousing are typically implemented as separate subsystems, which can limit system throughput, data transparency, and product traceability. This study proposes a supervisory integration framework that links AOI-based inspection and robotic handling with barcode-assisted warehousing through a PC-based supervisory application coupled with a centralized relational database. The main contribution is a unified inspection-to-warehousing workflow that associates AOI outcomes, product identity, storage contents, and warehousing status within a synchronized relational record, enabling a consistent linkage between physical printed circuit boards (PCBAs) and digital production data. The platform was implemented on a laboratory-scale SMT pilot line using an industrial AOI sensor, an industrial robot for physical handling operations, a barcode reader for product identification, and a supervisory application, implemented in C# WinForms, for integration and visualization. Experimental validation included AOI inspection of 512 PCBAs and barcode identification of 200 storage boxes under laboratory conditions. Experimental results showed that the AOI module achieved 95.2% classification accuracy for qualified boards and an 88.2% detection rate for defective units, while the barcode module successfully identified 97.5% of storage boxes on the first pass. The integration synchronization enabled automatic generation of warehousing records without manual data entry. These results support the feasibility of the proposed integration approach for enabling traceability and operational consistency in SMT production. Validation is limited to a laboratory-scale configuration, and larger-scale throughput and database stress testing remain future work.

1. Introduction

In the past few decades, the rapid growth of smart electronic devices—ranging from mobile products to Internet of Things (IoT) applications and industrial embedded systems—has increased demand for compact, reliable, and high-performance printed circuit board assemblies (PCBAs). Surface mount technology (SMT), pioneered in the 1960s to overcome the limitations of traditional through-hole technology [1], [2], has since become the dominant manufacturing paradigm. By enabling the direct placement of components onto the board, SMT supports high component density and tight geometric tolerances that are essential for scalable electronics manufacturing [3]. As device complexity increases, enabling consistent PCBA functional efficiency and traceability across manufacturing and logistics has become increasingly important.

In general, the production flow of a PCBA passes through multiple complex and rigorous stages: (i) assembly and inspection, where electronic components are attached to the board and visible assembly quality is verified [4]–[15]; (ii) electrical and functional testing, which validates electrical connectivity and operating behavior of the board [16]–[19]; and (iii) post-production, where products are sorted, packaged, stored, and prepared for integration or shipment [20]–[22]. Within this workflow, automated optical inspection (AOI) serves as an image-based quality check that detects visible assembly defects, such as missing, shifted, or incorrectly oriented parts [23]–[25]. Typically, this subsystem integrates a high-resolution imaging sensor with associated lighting to evaluate PCB images, thereby helping maintain production quality in electronics manufacturing [26], [27].

After production testing, PCBAs enter the post-production stage, where sorting, labeling, packaging, warehousing, and inventory management are performed. Although this stage is critical for storage integrity and traceability, conventional industrial SMT lines often rely on manual intervention or loosely coupled subsystems [28]–[30]. As a result, product identification, storage records, and inspection results are often maintained separately, requiring manual data entry and reconciliation. This lack of integration makes it difficult to synchronize production and inventory data, which is a fundamental requirement of modern, data-driven supply chains [31]–[33].

Several studies have investigated individual segments of the PCBA workflow; however, end-to-end linkage across inspection, handling, and warehousing remains limited. In AOI research, a variety of PCB defect detection methods have shifted from traditional rule-based or hand-crafted vision pipelines to optimized deep-learning detectors (e.g., YOLO-family variants [34], [35] and pyramid-based architectures [36]) to improve detection accuracy and inference speed under practical factory conditions [37]–[41]. While such studies enhance robustness to small defects and illumination variation, they typically treat AOI as an isolated inspection stage that outputs defect decisions without addressing how inspection outcomes are synchronized with subsequent handling actions and warehouse records.

Similarly, vision-integrated robotic systems have been proposed for automated handling and sorting of PCBAs based on visual classification results [42]–[45]. The cameras in these applications can be equipped directly on the robotic arms to provide flexible and close-up visual feedback [42], [43], [46], or located in a static position relative to the robot's workspace to provide a consistent field of view for monitoring or quality control [47]. However, these systems are evaluated as standalone operational units, and the reported contributions primarily focus on vision–robot control integrations rather than data integration mechanisms that preserve product identity across inspection, physical handling, and inventory updates.

In automated warehousing environments, standardized identification mechanisms are commonly employed to associate physical storage units with digital inventory records, including 1D/2D barcode (QR/Data Matrix) scanning incorporated with automated guided vehicles (AGVs) [48]–[51], RFID-based identification [52]–[55], and vision-assisted label recognition [56]–[59]. Among these methods, barcode-assisted identification remains particularly attractive in industrial settings owing to its low implementation cost, well-developed nature, and ease of integration with database-driven warehouse management systems. Therefore, this study adopts barcode technology in the warehousing stage.

From a logistics and data-management perspective, many electronics manufacturing deployments still maintain production and warehouse information in separate software systems. Inspection tools and equipment controllers typically record quality and handling events [60]–[62], whereas enterprise applications—such as Manufacturing Execution System (MES), Enterprise Resource Planning (ERP), and Warehouse Management System (WMS)—store production orders, inventory status, and warehouse transactions in different databases [63]–[65]. Different identifiers and data formats across these systems require manual reconciliation to synchronize production and warehouse records. Consequently, inspection decisions are not automatically linked to the specific storage identities and the associated import/export updates, leading to potential record inconsistencies and reducing end-to-end traceability.

To address this gap, the present study develops a supervisory integration framework that links AOI-based inspection, robotic handling, and barcode-assisted warehousing through a PC-based application and a centralized relational database. Rather than treating inspection, handling, and storage as separate events, the proposed workflow maintains a synchronized mapping among AOI outcomes, decoded product identity, stored contents, and warehousing status. In this method, the PC-based supervisory application performs the synchronization logic for record generation, whereas the database serves as the authoritative data layer for persistent storage and supports the relational linkage between physical PCBAs and digital production records.

The research contributions are as follows:

- A supervisory integration framework that links AOI inspection, robotic handling, barcode-based box identification, and warehousing record generation within one traceability workflow.
- A closed-loop synchronization mechanism that preserves the association among AOI results, product identity, stored contents, and stock status in a single transactional update.
- A laboratory-scale implementation and validation using an industrial AOI sensor, industrial robot, barcode reader, and PC-based supervisory application interfaced with a centralized relational database.

The remainder of this paper is organized as follows. Section 2 presents the proposed integration framework, including automated optical inspection, barcode-assisted warehousing, and supervisory data management. Section 3 describes the laboratory-scale experimental setup and hardware configuration. Section 4 reports and discusses the results obtained. Section 5 concludes the paper with its main findings, limitations, and future work.

2. Materials and Methods

This study follows a design–implementation–validation process consisting of three phases. First, the system architecture for the proposed supervisory integration framework is defined. This is followed by the implementation of the framework on a laboratory-scale SMT pilot line that integrates an AOI sensor, an industrial robot, and a barcode reader with a PC-based supervisory application and a centralized relational database. Finally, the framework is validated through closed-loop experiments and transactional record verification, with particular focus on inspection, product identification, and system-level synchronization. The overall research methodology is illustrated in Fig. 1.

The following subsections describe the specific components of the system architecture, including the hardware modules and the supervisory integration platform. Detailed specifications are also provided for the communication interfaces and the closed-loop operation protocols that coordinate the production flow. Lastly, the timing configurations established for the pilot line implementation are introduced to support the evaluation of the integrated synchronization logic.

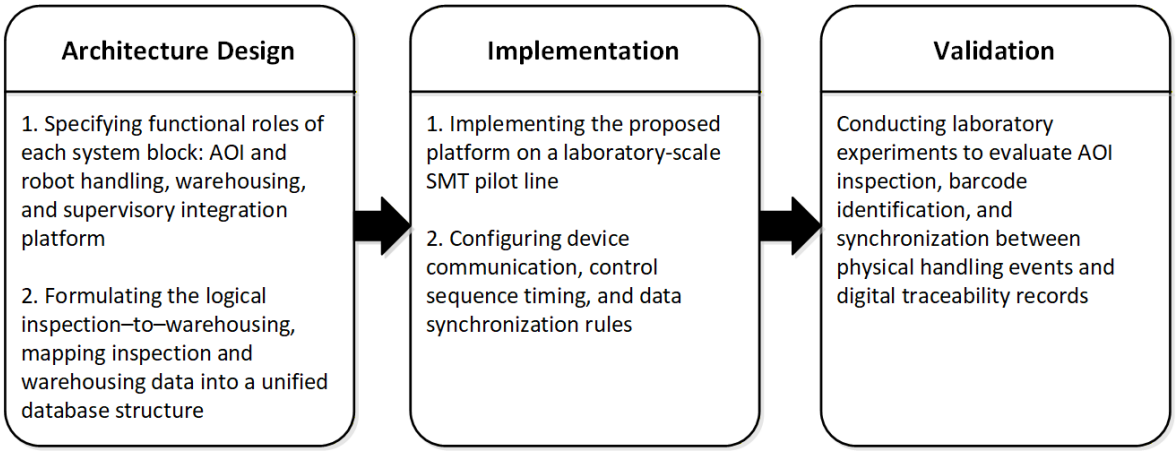

Fig. 1. Research methodology workflow

2.1. System Architecture

The proposed approach integrates three functional elements: (i) an AOI-based inspection and robotic handling module, (ii) a barcode-assisted automated warehousing subsystem, and (iii) a PC-based supervisory application connected to a centralized relational database for traceability and synchronization. Fig. 2 shows the system architecture, in which the supervisory application acquires data from both the AOI—robot handling and the warehousing modules and stores the corresponding records in the database. In this proposed framework, the supervisory application serves as the integration middleware at runtime, while the database functions as the centralized system of record for synchronized, traceable, and queryable data. The robotic handling sequence is coordinated by a programmable logic controller (PLC) based on AOI outcomes.

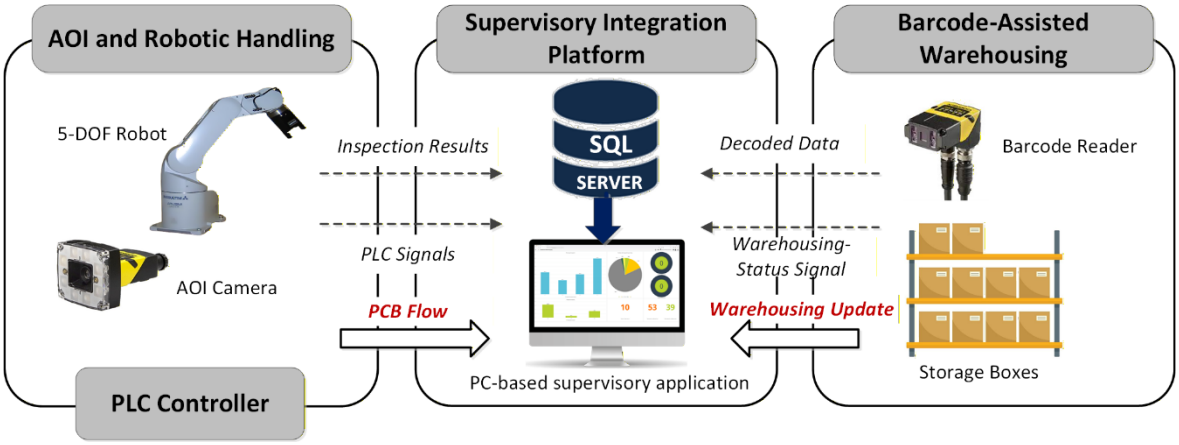

Fig. 2. Architecture of the proposed framework. The dashed arrows represent information flow, while the thick arrows depict physical flow

To evaluate the feasibility of the proposed platform, a laboratory-scale SMT pilot line was developed. Fig. 3 shows the front-side three-dimensional layout of the pilot line with the spatial arrangement of the AOI station, robot workspace, PLC control cabinet, and system supervisory PC. The barcode scanning area is located at the rear of the line, as indicated in the figure. In the pilot line, a simulated warehouse with multiple floors of slots for storage boxes is arranged inside the control cabinet. The warehousing transfer unit is implemented using a custom-developed XYZ Cartesian gantry robot integrated with PLC control. Since the focus of this study is the integration and synchronization framework rather than the mechanical design of the gantry system, detailed design and motion-control analysis of the gantry robot are outside the scope of this paper.

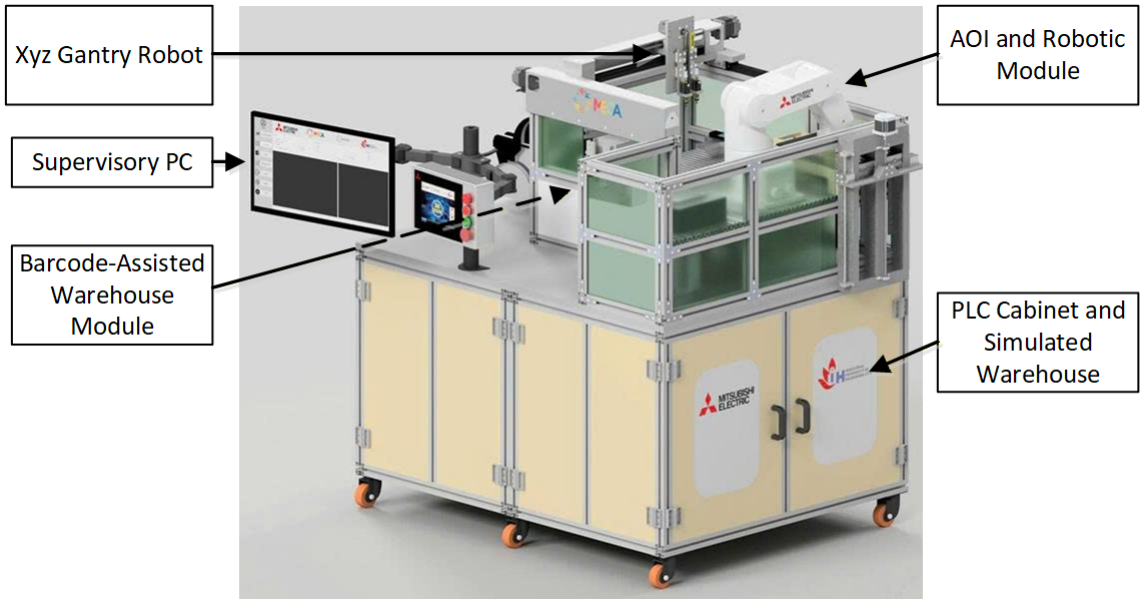

Fig. 3. Three-dimensional front view of the laboratory-scale SMT assembly line (overall dimensions: 110 × 130 × 190 cm, width × length × height)

2.2. AOI-Based Inspection and Robotic Handling Module

The AOI-based inspection and robotic handling module, designed for visual inspection and physical handling, is equipped with a five-degree-of-freedom (5-DOF) industrial robot (RV-2AJ, Mitsubishi, Japan) and an industrial imaging sensor (In-Sight 2001M, Cognex, USA). The sensor is mounted above the robot gripper (Fig. 4) to capture monochrome VGA images (640×480) of the boards under test. The robot transports PCBAs to an inspection station immediately after the assembly stage (Fig. 5) and performs robotic handling, including sorting PCBAs into designated storage boxes based on inspection results.

The AOI module is configured to detect three representative defect types:

(i) missing components, characterized by the absence of one or more components from their designated positions,

(ii) component misalignment, defined as the positional offset with the tolerance of ±0.3 mm between the actual component centroid and the computer-aided design (CAD) reference, and

(iii) angular misalignment, identified when a component is rotated relative to the contact pads beyond a specific threshold that is restricted to ±5° for large components and ±3° for two-pin parts.

AOI inspection was implemented within the Cognex In-Sight Explorer environment using Regions-of-Interest (ROI)-based pattern tools. Initially, the global Locate Part tool was utilized to localize a batch of six PCBAs at the inspection station per cycle. Subsequently, the pattern-matching algorithm of the Inspect Part tool was applied to each component to evaluate its presence, positional offset, and angular deviation. The acceptance threshold, representing the minimum pattern-match score, was set to 50/100. Consistent with the defect definitions, the rotation-tolerance parameters for angular misalignment were maintained at ±5° and ±3°, depending on the component type.

Inspection results are categorized as OK or NG, corresponding to qualified and defective boards, and are subsequently transmitted to an R04EN PLC (Mitsubishi, Japan) to guide the robot's motion. The PLC coordinates the inspection-to-handling sequence by receiving AOI outcomes and issuing commands to the robot and peripheral devices. In the pilot line, the PLC controller cabinet is arranged in the lower section (Fig. 3).

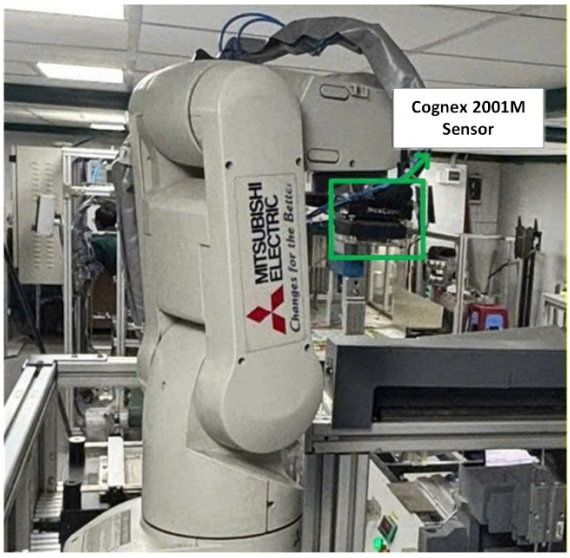

Fig. 4. Arrangement of the AOI-based inspection and robot handling module

2.3. Barcode-Assisted Automated Warehousing Module

The warehousing subsystem identifies storage boxes using a barcode reader (DataMan DM262Q, Cognex, USA). Following AOI inspection, the Mitsubishi robot sorts PCBAs into storage boxes on two distinct trays in the pilot line, representing Pass and Fail categories. Each box is preprinted with a unique one-dimensional barcode that identifies its production batch and contents.

A customized PLC-controlled XYZ gantry robot, as shown in Fig. 3, is employed to perform automated storage and retrieval operations within the warehouse grid. In addition, an optical sensor (WL4SLG-3P2232, SICK, Germany) is mounted behind the reader to detect when storage boxes are placed in the simulated warehouse. The sensing signal is used to trigger data synchronization at the supervisory integration platform, which is detailed in the following subsection.

Fig. 5 shows the rear-side arrangement of the warehousing subsystem in the pilot model. The barcode reader is clearly positioned in the figure, whereas the optical sensor and simulated warehouse are situated beneath and thus are not fully visible in this view. Additionally, the inspection station integrated with the AOI module is located at the rear of the model, also shown in the figure.

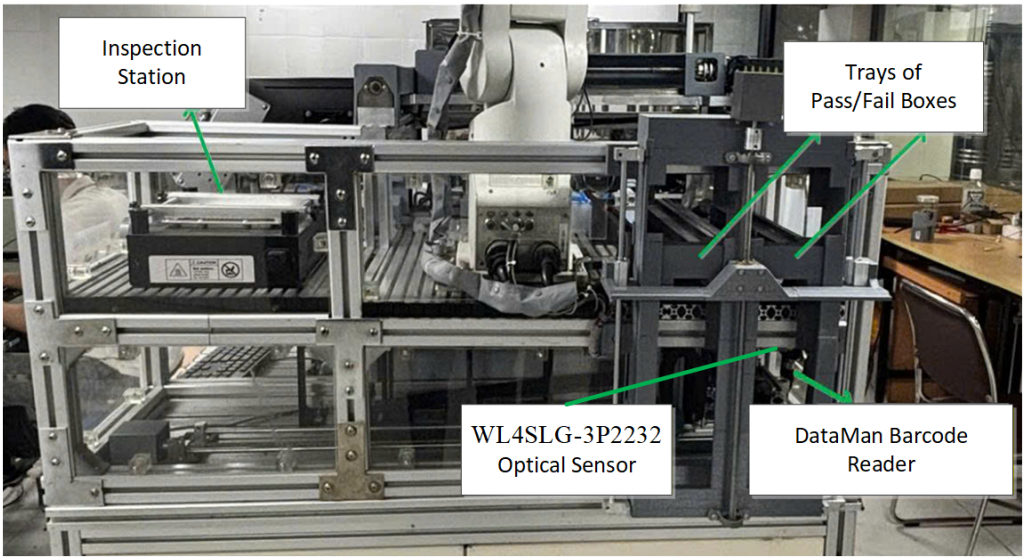

Fig. 5. Rear-side view of the automated warehousing subsystem. The inspection station is located immediately after the assembly stage

2.4. PC-Based Supervisory Integration Platform

The PC-based supervisory platform plays a central role in the proposed framework by coordinating data synchronization, traceability management, and record generation across the inspection and warehousing stages. The platform comprises two main components: a PC-based supervisory application developed in C# WinForms and a relational database implemented in Microsoft SQL Server. Within this architecture, the supervisory application functions as the transactional backbone of the system, where AOI inspection events, storage operations, and inventory updates are associated and written to the database.

The SQL database serves as the central repository for synchronized traceability information generated during system operation. These records include AOI inspection results, storage box identities and contents, and stock status (in-stock/out-of-stock). SQL Server is therefore used to store and retrieve traceability records for reporting and inventory queries.

This supervisory integration design was selected for the present laboratory-scale pilot model because it provides a straightforward implementation and reliable management of synchronized records within a unified platform. By integrating event coordination within the supervisory application and persistent storage in the relational database, the platform supports consistent traceability without the need for complex architecture. For larger-scale or distributed deployments, future work may consider extending this design through publish–subscribe middleware such as Message Queuing Telemetry Transport (MQTT) or Data Distribution Service (DDS).

2.5. Data Exchange and Synchronization Mechanism

This subsection details the multi-protocol communication used for subsystem integration, as illustrated in Fig. 6. The PC-based supervisory application communicates with the AOI sensor and barcode reader via the In-Sight Software Development Kit (SDK) version 6.5.1 and DataMan SDK version 5.6.0, respectively. Using the vendor SDKs shortens development time while ensuring system compatibility and stable operation during deployment.

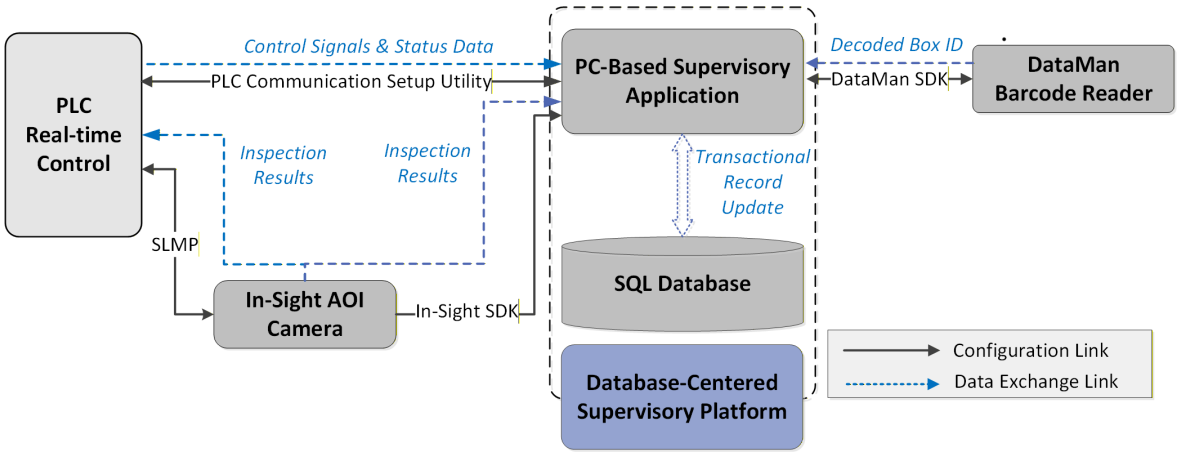

Fig. 6. Configuration of data exchange and synchronization

To establish communication between the Mitsubishi PLC and the supervisory interface, PLC parameters are defined using the Communication Setup Utility tool within the MX Component software (Mitsubishi, Japan). The connection is facilitated via Ethernet using the User Datagram Protocol/Internet Protocol (UDP/IP) protocol with a static IP address. Concurrently, AOI outcomes are transmitted to the PLC through the Seamless Message Protocol (SLMP), triggering the PLC to execute downstream robotic handling. As the communication bridge among the PLC, the two vision subsystems, and SQL Server, the supervisory application eliminates the necessity of additional dedicated communication hardware in the proposed platform.

The synchronization mechanism of the proposed supervisory integration framework is performed at the box level by generating a consistent mapping between AOI outcomes and the destination storage box identity. For each tested batch of PCBAs, the C# WinForms supervisory application records an inspection record (batch image, OK/NG, timestamp) and assigns it to the current destination box selected by the PLC (Pass/Fail). A box record is created and updated when the box barcode is decoded, providing a unique box identifier and other contents such as board type. The supervisory application then updates the box-contents record by appending the inspected batch assigned to that box and updates the stock status field (e.g., in-stock/out-of-stock). These updates are written to SQL Server as a single transactional update to ensure that the AOI outcome, box identity, box contents, and stock status remain consistent in the database.

2.6. Closed-Loop System Operation

The operation of the proposed platform follows a closed-loop inspection-to-warehousing workflow as follows:

(i) AOI inspection: After the assembly stage, the AOI camera captures images of the PCBAs (a batch of six boards per inspection cycle) and evaluates component presence/absence, position, and orientation. The AOI module then produces an OK/NG outcome for the batch, along with six classification results corresponding to each board.

(ii) PLC-guided robotic handling: AOI outcomes are transmitted to the PLC, which selects the destination category for the inspected batch. The Mitsubishi robot then transfers the batch to the designated Pass or Fail box accordingly. In the pilot setup, each storage box is configured to receive three batches before the warehousing step is triggered.

(iii) Barcode-assisted warehousing: Before warehousing, each storage box is labeled with a unique barcode. The PLC-controlled gantry transfers the box to the barcode-scanning position, where the barcode reader decodes the box identity and transmits it to the C# WinForms supervisory application. The gantry then moves the box to the simulated warehouse, and the optical sensor generates a warehousing-status signal to the supervisory platform to confirm storage.

(iv) Database synchronization: The supervisory application collects AOI outcomes and box identities. Immediately after receiving the warehousing-status signal, the supervisory application associates AOI outcomes and box identities with stock status, from which other product information, including box categories (Pass or Fail), board type, and quantity of qualified and defective boards per box, is extracted. These details are then stored in SQL Server, enabling traceability queries and inventory reporting.

2.7. Implementation Parameters and Timing Configuration

All tasks were configured to operate under timing constraints representative of the closed-loop inspection-to-handling process. The average duration and maximum allowable delay were specified for each task of the pilot line. These timing parameters are summarized in Table 1.

The key highlights of this configuration include:

- System synchronization: The AOI camera and the Mitsubishi robotic arm are synchronized with a low deviation (under 50 ms), ensuring the robot receives control commands immediately after an inspection result is generated.
- Data transmission: Inspection data and sorting results are exchanged between the AOI camera, PLC, and supervisory application within 10–150 ms, supporting a deterministic control workflow.
- Database integration: Applying non-blocking transactions and an average timing of 15 ms for recording information into the SQL database is sufficient for a laboratory-scale deployment to avoid observable interference with the pilot-line workflow.

- Retry mechanism: If a signal is interrupted within a predefined timeout, the supervisory application automatically re-sends the request up to three times before issuing an error notification.

Table 1. Timing configuration of the pilot line

Operation	Description	Average Duration	Maximum Allowable Delay	Note
AOI Inspection	Visual inspection duration	150 ms	160 ms	—
AOI Camera—Supervisory application	Transmission of inspection records from the AOI camera to the supervisory application	10 ms	20 ms	Configured via In-Sight SDK
AOI Camera—PLC	Transmission of inspection results from the AOI camera to the PLC	150 ms	160 ms	Configured via SLMP (Ethernet)
Robot handling actions	Box sorting duration by the robot	1.8 s	1.95 s	The sorting time per board
Barcode reading	Barcode scanning and decoding duration	120 ms	125 ms	1-D barcode recognition
Barcode reader—Supervisory interface	Transmission of decoded information from the barcode reader to the supervisory application	10 ms	20 ms	Via DataMan SDK
SQL Server	Database latency for record insertion	15 ms	25 ms	Non-blocking transactions applied
Signal synchronization deviation	Synchronization deviation between AOI output and PLC/Robot trigger	< 50 ms	—	No frame misalignment detected
Timeout/packet loss	Configured timeout/packet loss	< 0.1 %	—	Retry mechanisms applied
System availability	System uptime during the production phase	99.5 %	—	Excluding scheduled maintenance

3. Experimental Methods

3.1. Experimental Setup

Three experiment groups were carried out on the laboratory-scale SMT pilot line to evaluate the proposed platform:

(i) AOI inspection performance,

(ii) barcode-assisted identification, and

(iii) database synchronization.

For AOI validation, a total of 512 PCBAs were tested, comprising 478 qualified boards and 34 defective boards that were intentionally generated. For barcode validation, 200 storage boxes with one-dimensional barcode labels were processed. In addition, system synchronization and communication behavior were demonstrated using configured response-time and delay constraints for AOI, PLC communication, barcode decoding, and SQL response. All experiments were conducted under laboratory conditions with ambient lighting levels ranging from 400 to 600 lx and moderate dust levels.

3.2. Experimental Configuration and Calibration for Reproducibility

To ensure reproducible inspection and handling, the pilot line was configured with a fixed camera board geometry and repeatable positioning of PCBAs at the inspection station. The AOI sensor was calibrated by (i) setting a stable imaging configuration with a focus of 150 mm, exposure of 10 ms, and 1.0x gain, (ii) maintaining constant lighting conditions using warm-yellow LEDs within the laboratory environment, and (iii) defining a consistent field of view (FOV) centered on the target components. Within this FOV, the spatial layout for the six PCBA units was strictly mapped to ensure full coverage while minimizing perspective distortion.

The robotic handling was performed using the Mitsubishi RV-2AJ industrial arm, with a position repeatability of ±0.02 mm, ensuring consistent placement at the inspection station. The robot was calibrated by teaching specific pick, inspection, and placement poses relative to the inspection station and the locations of the Pass/Fail boxes. These trajectories were managed via PLC sequencing to ensure deterministic cycle times and consistent box assignment. For the warehousing subsystem, barcode labels were standardized in size and contrast, and the reader was configured with Code 128 symbology and an 8-ms exposure time to guarantee reliable decoding at the designated scan distance and angle.

3.3. Evaluation Metrics

To evaluate AOI performance through multiple categories, we propose using the following metrics:

- Quality Acceptance Rate (QAR), denoting the percentage of non-defective (OK) boards correctly identified by the system out of the total qualified population:

$$QAR = \frac{Correctly\ classified\ qualified\ boards}{Total\ qualified\ boards} \quad (1)$$

- Category-Specific Recall (CSR), indicating the detection accuracy calculated for an individual defect class, such as missing components or angular misalignment:

$$CSR = \frac{Correctly\ detected\ boards\ in\ category\ i}{Total\ tested\ boards\ in\ category\ i} \quad (2)$$

- Total Defect Recall (TDR), representing the proportion of all defective (NG) boards successfully detected by the AOI module:

$$TDR = \frac{Correctly\ detected\ defective\ boards}{Total\ defective\ boards} \quad (3)$$

- In addition, the performance of the barcode-based identification was evaluated using the first-pass read rate (FPRR), defined as:

$$FPRR = \frac{Number\ of\ boxes\ decoded\ succesfully\ on\ the\ first\ reading}{Total\ number\ of\ tested\ boxes} \quad (4)$$

4. Results and Discussion

4.1. Performance of AOI-Based Inspection

Following the configuration detailed in Subsection 2.2, the AOI module was evaluated against three defect categories: (1) missing components, (2) component misalignment, and (3) angular misalignment. Among the 512 PCBAs evaluated, 10 instances were prepared for missing components, 15 for component misalignment, and 9 for rotational misalignment. The detailed results outlining the detection rates and overall performance metrics for these three categories are presented in Table 2.

Table 2. AOI-based inspection performance

Defect Categories	Count of Boards Under Test	Count of Boards Detected	Metrics
Qualified (OK)	**478**	**455**	**QAR=95.2%**
Defective (NG)	**34**	**30**	**TDR=88.2 %**
Missing component	10	9	CSR_1=90.0%
Component misalignment	15	14	CSR_2=93.3%
Angular misalignment	9	7	CSR_3=77.8%

Accordingly, the QAR of 95.2% (455/478) indicates that the AOI module correctly identified a large majority of qualified products under the tested conditions. This high rate suggests a relatively low false-rejection tendency in the present setup. From a safety and quality perspective, the TDR of 88.2% (30/34) demonstrates overall sensitivity to manufacturing faults. Analysis of CSR reveals higher detection rates for component misalignments (93.3%) and missing components (90.0%) compared to angular misalignment (77.8%).

The lower recall for angular misalignment is primarily attributable to ambient lighting fluctuations, as the experiments lacked a strict lighting-control mechanism. The limited spatial resolution of the AOI sensor imposed inherent constraints on the capture of fine-grained pattern discrimination in small two-pin components. The performance variation also indicates that the current ROI-based thresholding vision algorithm is less sensitive to rotational deviations than to structural changes, such as missing parts.

Fig. 7 illustrates the graphical user interface (GUI) of the AOI inspection module during an active inspection cycle. The outermost green boundary defines the camera FOV, capturing the monochrome VGA image of a patch of six PCBAs placed on the top of the inspection station. Within this FOV, an internal green rectangle identifies the localized inspection zone for the batch. The small green markers superimposed on each board surface indicate the successful execution of the pattern-matching algorithm for individual components. The classification results are displayed simultaneously in the GUI for operational monitoring. In this example, all boards are indicated as “OK”, resulting in an overall "OK" classification for this batch.

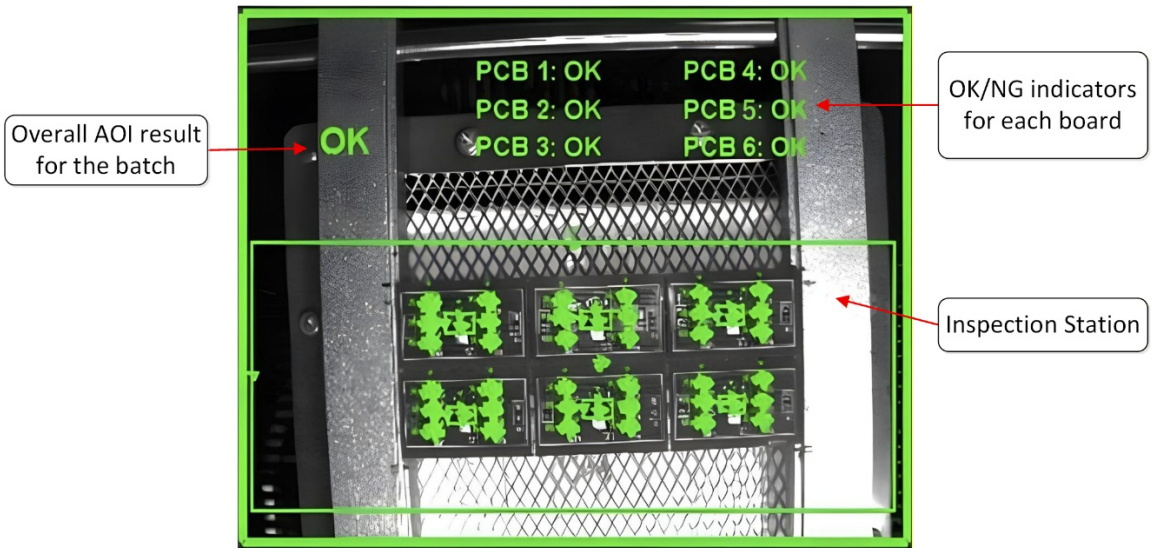

Fig. 7. AOI inspection display during an inspection cycle. The outermost green box represents the camera FOV, while the inner box defines the localized inspection zone for a batch of six PCBAs

4.2. Performance of Barcode-Assisted Identification

The barcode-assisted identification module was evaluated under representative laboratory warehousing conditions to assess the robustness of box-level data acquisition during storage operations. To emulate practical variability in warehousing, barcode labels were intentionally placed with rotational deviations of up to ±15° and minor horizontal offsets relative to the optical axis of the reader. These conditions were introduced to examine whether the identification process remained reliable prior to each storage event.

The box-transfer speed of the three-axis gantry robot was set within the range of 0.2 to 0.4 m/s to maintain consistency with the timing constraints of the closed-loop system, as summarized in Table 1. Within this operating range, the total identification delay, consisting of approximately 120 ms for barcode decoding and 10 ms for data transmission, remained below the residence time of each box

within the camera field of view. This timing margin allowed barcode acquisition and data synchronization to be completed without interrupting warehousing operations.

Among the 200 storage boxes tested, 195 were successfully decoded on the first scan, yielding an FPRR of 97.5%. The unreadable cases were primarily associated with poor print quality, dusty or scratched box surfaces, and suboptimal scanning orientations. These results indicate that the barcode-based identification module can reliably support the proposed synchronization workflow within the tested operating range, provided that barcode printing quality and surface cleanliness are adequately maintained. Within the tested angular and transfer-speed ranges, the barcode-assisted identification module demonstrated stable first-pass decoding performance for closed-loop warehousing synchronization.

As illustrated in Fig. 8, the identification module provides both visual confirmation and digital logging of the decoding process. Fig. 8(a) shows the capture interface, wherein the barcode is successfully localized within a green ROI and the decoded string "101031010" is accurately extracted. Correspondingly, Fig. 8(b) demonstrates the communication log, in which the decoded result and associated data string are recorded sequentially. This synchronized feedback loop facilitates real-time monitoring of the identification sequence, thereby reducing the possibility of identification mismatches before the PCBA enters the warehousing sequence.

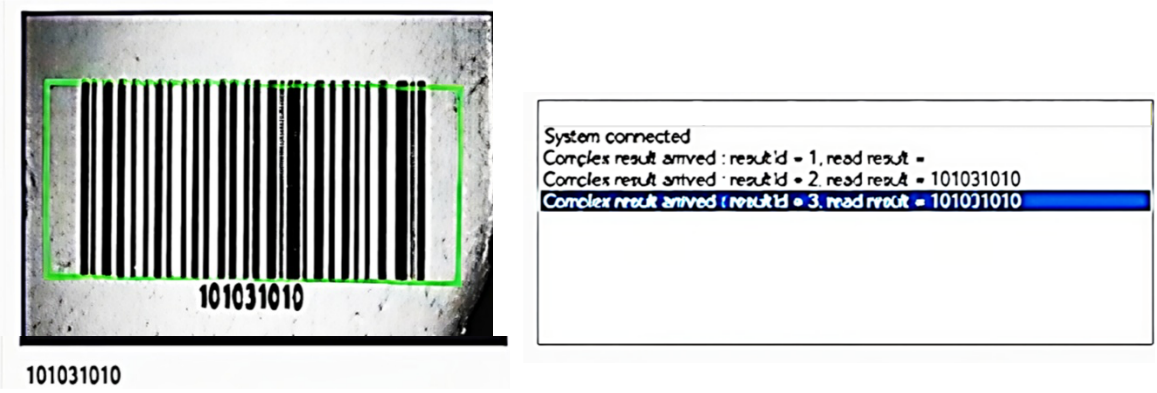

(a) (b)

Fig. 8. Decoding interface of the Cognex DataMan reader: (a) Scanner view showing the located 1-D barcode region (the green box). The decoded box identity is shown at the bottom; (b) The log output indicating successful decoding of the box identity (ID = 101031010)

4.3. Traceability Record Synchronization and Retrieval

This section examines how the proposed supervisory platform supports the synchronization and retrieval of traceability associated with inbound and outbound warehousing operations. Following the designed workflow in Subsection 2.6, AOI inspection outcomes (OK/NG) are coordinated with a storage-box identity obtained from barcode decoding and with the warehousing-status signal indicating that the box has been stored. The PC-based supervisory application consolidates these inputs and writes synchronized records to the centralized SQL Server database at the box level, enabling consistent linkage between physical PCBAs and their corresponding digital records.

Fig. 9 shows the inbound database generated from synchronized inspection and warehousing data in SQL Server. The table illustrates box-level records populated automatically by the PC-based supervisory application after AOI inspection and barcode identification, where “Product_Code” denotes box identifier, “Product_Name” identifies the type of the boards, “Date” presents the storage date, “Quantity” shows the quantity of qualified PCBAs per box, “Description” explains whether this box contains OK or NG batches (with the quantity of detected NG boards of the box in the latter case), and finally “Status” displays warehousing status (in-stock/out-of-stock).

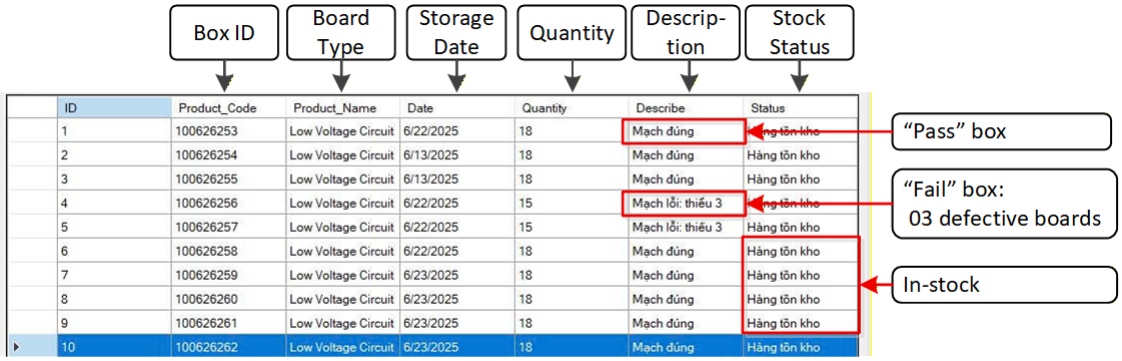

ID	Product_Code	Product_Name	Date	Quantity	Describe	Status
1	100626253	Low Voltage Circuit	6/22/2025	18	Mạch đúng	Hàng tồn kho
2	100626254	Low Voltage Circuit	6/13/2025	18	Mạch đúng	Hàng tồn kho
3	100626255	Low Voltage Circuit	6/13/2025	18	Mạch đúng	Hàng tồn kho
4	100626256	Low Voltage Circuit	6/22/2025	15	Mạch lỗi: thiếu 3	Hàng tồn kho
5	100626257	Low Voltage Circuit	6/22/2025	15	Mạch lỗi: thiếu 3	Hàng tồn kho
6	100626258	Low Voltage Circuit	6/22/2025	18	Mạch đúng	Hàng tồn kho
7	100626259	Low Voltage Circuit	6/23/2025	18	Mạch đúng	Hàng tồn kho
8	100626260	Low Voltage Circuit	6/23/2025	18	Mạch đúng	Hàng tồn kho
9	100626261	Low Voltage Circuit	6/23/2025	18	Mạch đúng	Hàng tồn kho
10	100626262	Low Voltage Circuit	6/23/2025	18	Mạch đúng	Hàng tồn kho

Fig. 9. Inbound (storage) record view. For Vietnamese strings, English translations are provided in callouts

Fig. 10 shows the outbound record view used to demonstrate retrieval/issuance record management, where product fields such as box identifier, board type, and stock status are retrieved from SQL Server and populated without manual re-entry. Other fields contain outgoing information about products that have been exported from the warehouse. Together, these views confirm that AOI outcomes and storage contents are consistently mapped into structured database records that can be queried for traceability and inventory reporting.

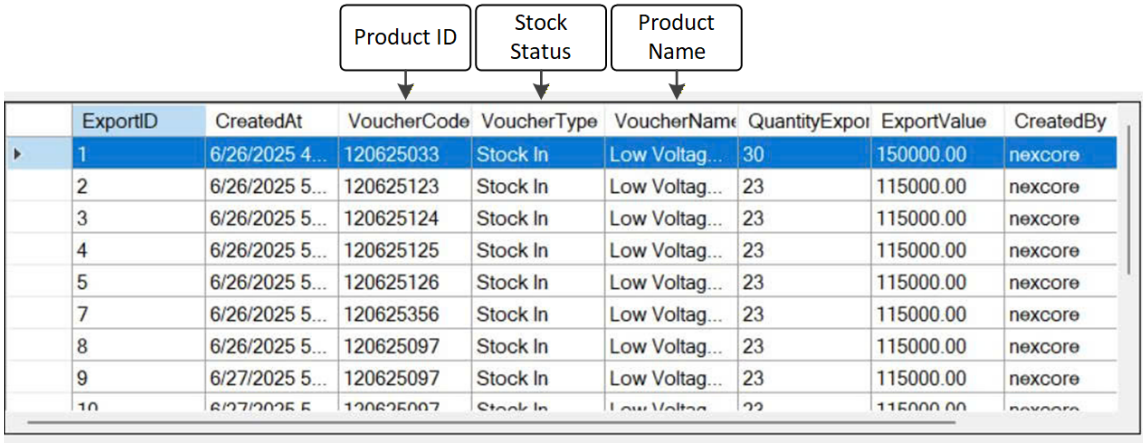

ExportID	CreatedAt	VoucherCode	VoucherType	VoucherName	QuantityExpor	ExportValue	CreatedBy
1	6/26/2025 4...	120625033	Stock In	Low Voltag...	30	150000.00	nexcore
2	6/26/2025 5...	120625123	Stock In	Low Voltag...	23	115000.00	nexcore
3	6/26/2025 5...	120625124	Stock In	Low Voltag...	23	115000.00	nexcore
4	6/26/2025 5...	120625125	Stock In	Low Voltag...	23	115000.00	nexcore
5	6/26/2025 5...	120625126	Stock In	Low Voltag...	23	115000.00	nexcore
7	6/26/2025 5...	120625356	Stock In	Low Voltag...	23	115000.00	nexcore
8	6/26/2025 5...	120625097	Stock In	Low Voltag...	23	115000.00	nexcore
9	6/27/2025 5...	120625097	Stock In	Low Voltag...	23	115000.00	nexcore
10	6/27/2025 5...	120625097	Stock In	Low Voltag...	23	115000.00	nexcore

Fig. 10. Outbound (export) record view (demonstration)

The successful generation and operation of these records demonstrate that inspection outcomes, storage identification, and box-level records are consistently maintained within a unified data pipeline. This consistency ensures data integrity across the production–logistics chain. Overall, the results demonstrate the feasibility of the proposed integration workflow for maintaining synchronized box-level traceability records in a laboratory-scale SMT environment.

5. Conclusion

This study introduced a supervisory integration framework that bridges the functional gap between automated optical inspection, robotic handling, and warehousing subsystems in SMT production. The primary theoretical contribution is a synchronized box-level traceability workflow that preserves the association among AOI outcomes, decoded box identity, box contents, and stock status in a relational database. This approach supports queryable traceability records across post-inspection handling and warehousing stages.

Experimental results on a laboratory-scale SMT pilot line demonstrated the feasibility and stability of the proposed approach. The AOI module achieved a Quality Acceptance Rate (QAR) of 95.2% and a Total Defect Recall (TDR) of 88.2%, while the barcode subsystem obtained a 97.5% first-pass read rate for product identification. In addition, the synchronization workflow enabled

automatic generation and retrieval of warehousing records from the database without manual re-entry, supporting operational consistency and traceability reporting.

The present validation is limited to a laboratory-scale configuration, and several limitations remain. The current AOI algorithm relies on rule-based pattern matching, which is sensitive to illumination variation and fine-angle defects, resulting in lower detection accuracy for rotational misalignment (77.8%). Additionally, the warehousing demonstration focuses on box-level records and does not evaluate large-scale warehouse operations or long-horizon database performance under week-scale production volumes. The timing parameters reported for closed-loop coordination are configured for demonstration rather than stress-tested under industrial throughput.

Future work should focus on improving robustness, scalability, and deployability of the proposed platform. The AOI pipeline can be extended from rule-based methods toward learning-based defect detection to improve sensitivity to small defects and fine rotational deviations, together with an enclosed inspection station for a stabilized illumination setting. The database should be stress-tested under high-volume workloads to measure update latency and to evaluate the benefits of advanced indexing and partitioning strategies for long-term traceability. Finally, to support distributed deployment across multiple production stations, the investigation of an event-driven publish-subscribe framework, such as MQTT or DDS, is recommended as a scalable alternative to the current centralized request-response model.

Author Contribution: All authors contributed equally to the main contributor to this paper. All authors read and approved the final paper.

Funding: This research received no external funding.

Acknowledgment: Not Applicable.

Conflicts of Interest: The authors declare no conflict of interest.

References

[1] H.-K. Wang, T.-Y. Yang, Y.-H. Wang, and C.-L. Wu, "Hybrid dispatching and genetic algorithm for the surface mount technology scheduling problem in semiconductor factories," *International Journal of Production Economics*, vol. 280, p. 109500, 2025, https://doi.org/10.1016/j.ijpe.2024.109500.

[2] G. Chen, G. Wang, Z. Wang, and L. Wang, "Electronic chip package and co-packaged optics (CPO) technology for modern AI era: A review," *Micromachines*, vol. 16, no. 4, p. 431, 2025, https://doi.org/10.3390/mi16040431.

[3] J. Wiklund, A. Karakoç, T. Palko, H. Yiğitler, K. Ruttik, R. Jäntti, and J. Paltakari, "A review on printed electronics: Fabrication methods, inks, substrates, applications and environmental impacts," *Journal of Manufacturing and Materials Processing*, vol. 5, no. 3, p. 89, 2021, https://doi.org/10.3390/jmmp5030089.

[4] A. Farrag, J. Kim, S. Yoon, and Y. Jin, "Detection of stencil printing direction in printed circuit boards assembly using solder paste inspection data," *The International Journal of Advanced Manufacturing Technology*, vol. 138, no. 1, pp. 97–112, 2025, https://doi.org/10.1007/s00170-024-14585-6.

[5] S. Jain, R. Patel, M. Desai, J.-P. Verma, and S.-W. Yoon, "Enhancing stencil printing in PCB production using deep learning based approach for residue classification and optimization," *International Journal of Information Technology*, vol. 17, no. 5, pp. 2971–2981, 2025, https://doi.org/10.1007/s41870-024-02392-x.

[6] R. Kaindl, D. Dergez, T. Gupta, S. Pei, P.-X. Hou, J. Du, C. Liu, B. Fickl, M. Nastran, Y. Liu, A. Blümel, D. Eder, J. Liu, W. Ren, P. Hartmann, W. Waldhauser, D. Kieslinger, and B.-C. Bayer, "Screen and stencil printed graphene heat spreaders on printed circuit boards for lowering of light emitting diode temperatures," *Surface and Coatings Technology*, vol. 517, p. 132821, 2025, https://doi.org/10.1016/j.surfcoat.2025.132821.

[7] C.-C. Lin and T.-N. Tsai, "Optimizing stencil printing parameters for multiple quality characteristics and diverse packages using a hybrid neural network and linear programming approach," *Soldering and Surface Mount Technology*, vol. 38, no. 1, pp. 32–49, 2025, https://doi.org/10.1108/SSMT-05-2025-0024.

[8] N. Cao, D. Won, and S.-W. Yoon, "PADS: Predictive anomaly detection for SMT solder joints using novel features from SPI and pre-AOI data," *IEEE Transactions on Components, Packaging and Manufacturing Technology*, vol. 14, no. 3, pp. 501–509, 2024, https://doi.org/10.1109/TCPMT.2024.3367244.

[9] C.-S. Chen, H. Wang, Y.-C. Kao, P.-J. Lu, and W.-R. Chen, "Predictive model of the solder paste stencil printing process by response surface methodology," *Soldering and Surface Mount Technology*, vol. 34, no. 5, pp. 292–299, 2022, https://doi.org/10.1108/SSMT-08-2021-0056.

[10] J. Xie, Y. Guo, D. Liu, S. Huang, K. Zheng, and Y. Tao, "A multimodal fusion method for soldering quality online inspection," *Journal of Intelligent Manufacturing*, vol. 36, no. 5, pp. 3271–3284, 2025, https://doi.org/10.1007/s10845-024-02413-3.

[11] J. He, Y. Cen, S. Alelaumi, and D. Won, "An artificial intelligence-based pick-and-place process control for quality enhancement in surface mount technology," *IEEE Transactions on Components, Packaging and Manufacturing Technology*, vol. 12, no. 10, pp. 1702–1711, 2022, https://doi.org/10.1109/TCPMT.2022.3215109.

[12] J. Kim, Z. Zhang, D. Won, S. Yoon, and Y. Jin, "A pick-and-place process control based on the bootstrapping method for quality enhancement in surface mount technology," *The International Journal of Advanced Manufacturing Technology*, vol. 133, no. 1, pp. 745–763, 2024, https://doi.org/10.1007/s00170-024-13767-6.

[13] S. Lima, L. Silva, A.-M. Gonçalves, M.-T. Malheiro, M. Pinhão, J. Machado, J. Meireles, and A.-J. Pontes, "Statistical methodologies for determining critical parameters in a pick-and-place process on a surface mount device line," *Research in Statistics*, vol. 3, no. 1, p. 2482648, 2025, https://doi.org/10.1080/27684520.2025.2482648.

[14] J.-R. Lee, M.-S.-A. Aziz, M.-H.-H. Ishak, and C.-Y. Khor, "A review on numerical approach of reflow soldering process for copper pillar technology," *The International Journal of Advanced Manufacturing Technology*, vol. 121, no. 7, pp. 4325–4353, 2022, https://doi.org/10.1007/s00170-022-09724-w.

[15] C.-H. Lee, K.-X. Lin, and C.-W. Chou, "Surrogate-based optimization framework for enhancing SMT process quality and productivity in electronics manufacturing services," *The International Journal of Advanced Manufacturing Technology*, vol. 136, no. 11, pp. 5103–5122, 2025, https://doi.org/10.1007/s00170-025-15032-w.

[16] E. Weiss, "Preventing corrosion-related failures in electronic assembly: A multicase study analysis," *IEEE Transactions on Components, Packaging and Manufacturing Technology*, vol. 13, no. 5, pp. 743–749, 2023, https://doi.org/10.1109/TCPMT.2023.3285776.

[17] T. Sindel, N. Thielen, F. Mahr, T. Reichenstein, H. Erdogan, and J. Franke, "Data-driven bed of nails wear analysis for the in-circuit-testing of electronic modules," in *Proceedings of the 2024 IEEE 29th International Conference on Emerging Technologies and Factory Automation (ETFA)*, 2024, pp. 1–6, https://doi.org/10.1109/ETFA61755.2024.10710880.

[18] J.-R. Deshmukh, G.-P. Kurien, and S.-K. Saha, "Process optimization using value stream mapping in PCB manufacturing," in *Proceedings of the 2022 International Conference on Trends in Quantum Computing and Emerging Business Technologies (TQCEBT)*, 2022, pp. 1–6, https://doi.org/10.1109/TQCEBT54229.2022.10041540.

[19] C. Wang, X. Xie, and H. Lyu, "A study on a PCBA short circuit detection method based on the Hall effect," in *Proceedings of the 2024 IEEE 4th International Conference on Information Technology, Big Data and Artificial Intelligence (ICIBA)*, 2024, pp. 1678–1684, https://doi.org/10.1109/ICIBA62489.2024.10868641.

[20] M.-A. Filz, J.-P. Bosse, and C. Herrmann, "Digitalization platform for data-driven quality management in multi-stage manufacturing systems," *Journal of Intelligent Manufacturing*, vol. 35, no. 6, pp. 2699–2718, 2024, https://doi.org/10.1007/s10845-023-02162-9.

[21] O. Makinde, R. Selepe, T. Munyai, K. Ramdass, and A. Nesamvuni, "Improving the supply chain performance of an electronic product-manufacturing organisation using DMAIC approach," *Cogent Engineering*, vol. 9, no. 1, p. 2025196, 2022, https://doi.org/10.1080/23311916.2021.2025196.

[22] I.-R. Puiu, I. M. Petre, and M. Boșcoianu, "Targeting toward optimal inventory in automotive industry-an analysis based on six sigma methodology," *Logistics*, vol. 10, no. 1, p. 8, 2026, https://doi.org/10.3390/logistics10010008.

[23] V. U. Sankar, G. Lakshmi, and Y. S. Sankar, "A review of various defects in PCB," *Journal of Electronic Testing*, vol. 38, no. 5, pp. 481–491, 2022, https://doi.org/10.1007/s10836-022-06026-7.

[24] K. Singh, S. Kharche, A. Chauhan, and P. Salvi, "PCB defect detection methods: A review of existing methods and potential enhancements," *Journal of Engineering Science and Technology Review*, vol. 17, no. 1, pp. 156–167, 2024, https://doi.org/10.25103/jestr.171.19.

[25] S. N. A and A. D. V. K, "AI-driven automated optical inspection for surface-mounted devices in printed circuit boards: A systematic review," in *Proceedings of the 2026 International Conference on Intelligent and Innovative Technologies in Computing, Electrical and Electronics (IITCEE)*, 2026, pp. 1–6, https://doi.org/10.1109/IITCEE67948.2026.11394611.

[26] P. Parlecha, S. Biswas, S. V. G, and T. V. Prabhakar, "Smart automated optical inspection of PCBs," in *Proceedings of the 2025 IEEE Physical Assurance and Inspection of Electronics (PAINE)*, 2025, pp. 1–7, https://doi.org/10.1109/PAINE66113.2025.11320200.

[27] T. Li, K. Qi, W. Liu, X. Yang, and H. Sun, "An efficient PCBA semantic segmentation network based on automated optical inspection," *Optics and Lasers in Engineering*, vol. 194, p. 109202, 2025, https://doi.org/10.1016/j.optlaseng.2025.109202.

[28] R. Seidel, B. Rachinger, N. Thielen, K. Schmidt, S. Meier, and J. Franke, "Development and validation of a digital twin framework for SMT manufacturing," *Computers in Industry*, vol. 145, p. 103831, 2023, https://doi.org/10.1016/j.compind.2022.103831.

[29] J. Chang, Z. Qiao, Q. Wang, X. Kong, and Y. Yuan, "Investigation on SMT product defect recognition based on multi-source and multi-dimensional data reconstruction," *Micromachines*, vol. 13, no. 6, p. 806, 2022, https://doi.org/10.3390/mi13060860.

[30] P.-E. Dossou, P. Torregrossa, and T. Martinez, "Industry 4.0 concepts and lean manufacturing implementation for optimizing a company logistics flows," *Procedia Computer Science*, vol. 200, pp. 358–367, 2022, https://doi.org/10.1016/j.procs.2022.01.234.

[31] A. Singh, A. Goel, A. Chauhan, and S. K. Singh, "Sustainability of electronic product manufacturing through e-waste management and reverse logistics," *Sustainable Futures*, vol. 9, p. 100490, 2025, https://doi.org/10.1016/j.sftr.2025.100490.

[32] Y. Pan, R. Y. Zhong, T. Qu, L. Ding, and J. Zhang, "Multi-level digital twin-driven kitting-synchronized optimization for production logistics system," *International Journal of Production Economics*, vol. 271, p. 109176, 2024, https://doi.org/10.1016/j.ijpe.2024.109176.

[33] L. C. Noal, B. T. Chaves, D. P. Lacerda, M. I. Motta Morandi, and F. A. S. Piran, "When inventories are not financial losses: A comparative analysis between lean and theory of constraints concepts for production synchronisation," *International Journal of Production Research*, pp. 1–23, 2025, https://doi.org/10.1080/00207543.2025.2577156.

[34] Z. F. Elsharkawy, "Enhanced YOLOv11 framework for high precision defect detection in printed circuit boards," *Scientific Reports*, vol. 15, no. 1, p. 42550, 2025, https://doi.org/10.1038/s41598-025-27415-w.

[35] G. Xiao, S. Hou, and H. Zhou, "PCB defect detection algorithm based on CDI-YOLO," *Scientific Reports*, vol. 14, no. 1, p. 7351, 2024, https://doi.org/10.1038/s41598-024-57491-3.

[36] K. C. Fung, K.-W. Xue, C.-M. Lai, K.-H. Lin, and K.-M. Lam, "Improving PCB defect detection using selective feature attention and pixel shuffle pyramid," *Results in Engineering*, vol. 21, p. 101992, 2024, https://doi.org/10.1016/j.rineng.2024.101992.

[37] Q. Ling and N. A. M. Isa, "Printed circuit board defect detection methods based on image processing, machine learning and deep learning: A survey," *IEEE Access*, vol. 11, pp. 15921–15944, 2023, https://doi.org/10.1109/ACCESS.2023.3245093.

[38] J. Lim, J. Lim, V. M. Baskaran, and X. Wang, "A deep context learning based PCB defect detection model with anomalous trend alarming system," *Results in Engineering*, vol. 17, p. 100968, 2023, https://doi.org/10.1016/j.rineng.2023.100968.

[39] G. G. de Oliveira, G. Caumo Vaz, M. Antonio Andrade, Y. Iano, L. Ronchini Ximenes, and R. Arthur, "System for PCB defect detection using visual computing and deep learning for production optimization," *IET Circuits, Devices and Systems*, vol. 2023, no. 1, p. 6681526, 2023, https://doi.org/10.1049/2023/6681526.

[40] Z. He, Y. Lian, Y. Wang, and Z. Lu, "A comprehensive review of research on surface defect detection of PCBs based on machine vision," *Results in Engineering*, vol. 27, p. 106437, 2025, https://doi.org/10.1016/j.rineng.2025.106437.

[41] V.-T. Nguyen, X.-T. Kieu, D.-T. Chu, X. Hoang Van, P.-X. Tan, and T.-N. Le, "Deep learning-enhanced defects detection for printed circuit boards," *Results in Engineering*, vol. 25, p. 104067, 2025, https://doi.org/10.1016/j.rineng.2025.104067.

[42] X. Yang, Z. Zhou, J. H. Sørensen, C. B. Christensen, M. Ünalan, and X. Zhang, "Automation of SME production with a cobot system powered by learning-based vision," *Robotics and Computer-Integrated Manufacturing*, vol. 83, p. 102564, 2023, https://doi.org/10.1016/j.rcim.2023.102564.

[43] T.-N. V., P.-T. Nguyen, S.-F. Su, P.-X. Tan, and T.-L. Bui, "Vision-based pick and place control system for industrial robots using an eye-in-hand camera," *IEEE Access*, vol. 13, pp. 25127–25140, 2025, https://doi.org/10.1109/ACCESS.2025.3536496.

[44] Y. Zhang and T. Wang, "Design of industrial robot sorting and assembly control system based on Profinet bus," *Frontiers in Mechanical Engineering*, vol. 11, p. 1635881, 2025, https://doi.org/10.3389/fmech.2025.1635881.

[45] F. J. Martínez-Peral, H. Migallón, J. Borrell-Méndez, M. Martínez-Rach, and C. Pérez-Vidal, "Manipulation order optimization in industrial pick-and-place operations: Application to textile and leather industry," *The International Journal of Advanced Manufacturing Technology*, vol. 133, no. 1, pp. 987–1010, 2024, https://doi.org/10.1007/s00170-024-13436-8.

[46] S. D'Avella, C. A. Avizzano, and P. Tripicchio, "ROS-industrial based robotic cell for Industry 4.0: Eye-in-hand stereo camera and visual servoing for flexible, fast, and accurate picking and hooking in the production line," *Robotics and Computer-Integrated Manufacturing*, vol. 80, p. 102453, 2023, https://doi.org/10.1016/j.rcim.2022.102453.

[47] U. Izagirre, I. Andonegui, L. Eciolaza, and U. Zurutuza, "Towards manufacturing robotics accuracy degradation assessment: A vision-based data-driven implementation," *Robotics and Computer-Integrated Manufacturing*, vol. 67, p. 102029, 2021, https://doi.org/10.1016/j.rcim.2020.102029.

[48] F. Alsulami and N. Z. Jhanjhi, "Deep learning framework for barcode localization and decoding using simulated UAV imagery," *Scientific Reports*, vol. 16, no. 1, p. 399, 2025, https://doi.org/10.1038/s41598-025-29720-w.

[49] B. Chen and J. Huang, "Drone-assisted QR code recognition method for warehouse management," in *Proceedings of the 2024 International Conference on Networking, Sensing and Control (ICNSC)*, 2024, pp. 1–6, https://doi.org/10.1109/ICNSC62968.2024.10760066.

[50] A. Belbachir, A. M. Ortiz, E. T. Hauge, A. N. Belbachir, G. Bonanno, E. Ciccia, and G. Felline, "Outdoor warehouse management: UAS-driven precision tracking of stacked steel bars," *SN Computer Science*, vol. 6, no. 6, p. 701, 2025, https://doi.org/10.1007/s42979-025-04206-8.

[51] A. Awasthi, P. Deepalakshmi, P. Nagaraj, and A. M. Vamsi, "Movable barcode scanning system using IoT smart glass technology," *International Journal of Intelligent Enterprise*, vol. 10, no. 2, pp. 113–124, 2023, https://doi.org/10.1504/IJIE.2023.130067.

[52] V. A. Manakova, N. N. Maiorov, and A. S. Kostin, "Routing models of autonomous unmanned system for solving problems in object identification at the warehouse," in *Proceedings of the 2025 Wave Electronics and Its Application in Information and Telecommunication Systems (WECONF)*, 2025, pp. 1–4, https://doi.org/10.1109/WECONF65186.2025.11017289.

[53] A. Kathiriya, "A review of RFID technology's impact on inventory management and supply chain optimization," *International Journal of Emerging Research in Engineering and Technology*, vol. 6, no. 3, pp. 86–94, 2025, https://doi.org/10.63282/3050-922X.IJERET-V6I3P110.

[54] Y. Zhang, Y. Lin, and A. Esfahbodi, "Digital transformations of supply chain management via RFID technology: A systematic literature review," *Journal of Digital Economy*, vol. 4, pp. 251–267, 2025, https://doi.org/10.1016/j.jdec.2025.06.001.

[55] G. Casella, S. Filippelli, B. Bigliardi, and E. Bottani, "Radio frequency identification technology in logistics: A review of the literature," *International Journal of RF Technologies*, vol. 12, no. 2, pp. 69–86, 2022, https://doi.org/10.3233/RFT-220321.

[56] H. Liu, L. Zhou, J. Zhao, F. Wang, J. Yang, K. Liang, and Z. Li, "Deep-learning-based accurate identification of warehouse goods for robot picking operations," *Sustainability*, vol. 14, no. 13, p. 7781, 2022, https://doi.org/10.3390/su14137781.

[57] C. Tadjine, A. Ouafi, A. Benlamoudi, and A. Taleb-Ahmed, "Computer vision in warehouse management automation: A survey on implemented methods with prototyping hardware," *Engineering Applications of Artificial Intelligence*, vol. 160, p. 111886, 2025, https://doi.org/10.1016/j.engappai.2025.111886.

[58] E. Flores-García, H. K. Dong, Y. Jeong, and M. Wiktorsson, "Machine learning in smart production logistics: A review of technological capabilities," *International Journal of Production Research*, vol. 63, no. 5, pp. 1898–1932, 2024, https://doi.org/10.1080/00207543.2024.2381145.

[59] J. Giner, D. Katic, K. Kovacs, R. Glawar, and W. Sihn, "A computer vision based approach to reduce system downtimes in an automated high-rack logistics warehouse," *Procedia CIRP*, vol. 118, pp. 1078–1083, 2023, https://doi.org/10.1016/j.procir.2023.06.185.

[60] F. Balaha, H. Albinali, H. Alrabiah, M. Ali, and Z. Bahroun, "An analytical review of data integration for decision support in smart manufacturing," *Decision Analytics Journal*, vol. 17, p. 100647, 2025, https://doi.org/10.1016/j.dajour.2025.100647.

[61] E. Rodriguez and A. J. Alvares, "Toward a digital ecosystem for additive manufacturing driven by standards-based digital thread and digital twins," *IEEE Access*, vol. 13, pp. 207776–207807, 2025, https://doi.org/10.1109/ACCESS.2025.3641205.

[62] P. Nguyen, M. Kim, E. Nichols, and H.-S. Yoon, "AI-driven digital twins for manufacturing: A review across hierarchical manufacturing system levels," *Sensors*, vol. 26, no. 1, p. 124, 2026, https://doi.org/10.3390/s26010124.

[63] N. Smina, Y. Gahi, and J. Gharib, "Data management in smart manufacturing supply chains: A systematic review of practices and applications (2020–2025)," *Information*, vol. 17, no. 1, p. 19, 2026, https://doi.org/10.3390/info17010019.

[64] T. Horak, P. Strelec, M. Kebisek, P. Tanuska, and A. Vaclavova, "Data integration from heterogeneous control levels for the purposes of analysis within Industry 4.0 concept," *Sensors*, vol. 22, no. 24, p. 9860, 2022, https://doi.org/10.3390/s22249860.

[65] G. Yasmeen, L. Anthonysamy, and A. O. Ojo, "Resource-governed BDA adoption for resilient supply-chain operations: Qualitative evidence from Malaysian manufacturing industry," *Sustainability*, vol. 17, no. 21, p. 9620, 2025, https://doi.org/10.3390/su17219620.